Supplemental Material

CRYSTAL STRUCTURE OF THE ENTIRE ECTODOMAIN OF GP130: INSIGHTS INTO THE MOLECULAR ASSEMBLY OF THE TALL CYTOKINE RECEPTOR COMPLEXES

Yibin Xu, Nadia J. Kershaw, Cindy S. Luo, Priscilla Soo, Michael J. Pocock, Peter E. Czabotar, Douglas J. Hilton, Nicos A. Nicola, Thomas P. J. Garrett, and Jian-Guo Zhang

Supplemental Methods

Generation of gp130 D1-D6 expression plasmid

pTriEx2 (Novagen) was digested with XcmI and XhoI and a synthetic DNA fragment encoding 5'-XcmI-His_6-FLAG-[TEV site]-XhoI-3' inserted by ligation independent cloning. A synthetic DNA fragment encoding baculovirus gp67 signal peptide was then inserted into the resultant vector using the NcoI site. This version of the vector was called pgpHFT, and encodes an N-terminal gp67 signal peptide, His_6 and Flag epitopes and a TEV cleavage site. DNA encoding the entire ectodomain of human gp130 D1-D6 (residues 1-597, note that the numbering system corresponds to the mature form of gp130 throughout this work) was cloned into pgpHFT to produce pgpHFT-gp130D1-D6.

Expression and purification of gp130-D1-D6

Sf21 insect cells were co-transfected with BacMagic baculovirus DNA (Novagen) and pgpHFT-gp130D1-D6 as per supplier's manual. The seed virus was amplified to obtain high-titre viral stocks, which were used to infect Sf21 cells. The supernatant was harvested and passed over anti-FLAG M2 agarose (Sigma). Bound protein was eluted with 300 μg/ml of FLAG peptide, concentrated with a 10-kDa MWCO centrifugal concentrator (Millipore) and applied to a Superdex 200 column (GE Healthcare) in 20 mM Tris-HCl, pH7.4, 100 mM NaCl. The tandem His_6 and FLAG tags were removed by digestion with TEV protease, followed by further gel filtration chromatography to remove the protease.

Expression and purification of gp130 D4-D6

DNA encoding amino acids 301 to 591 of human gp130 (D4-D6) was cloned into pET-Duet (Novagen) as an AscI/XhoI fragment, allowing expression of gp130 D4-D6 fused to an N-terminal His_6 tag. pET-Duet/gp130 D4-D6 was used to transform *E. coli* BL21(DE3) cells which were then grown at 37°C in Superbroth containing ampicillin at 100 μg/ml. When the OD_{600} reached 0.8, the temperature was lowered to 17°C. Protein expression was induced by addition of 1 mM isopropyl thio-β-D-galactoside and continued at 17°C overnight. Recombinant protein was isolated using Ni-NTA resin (Qiagen). Eluted protein was diluted 10-fold in 50 mM Tris-HCl, pH 7.5 (Buffer A) and applied to a MonoQ HR 5/5 (GE Healthcare) equilibrated in Buffer A. The flowthrough was concentrated and applied to a Superdex 200 column in Buffer A. Protein was concentrated to 2 mg/ml and stored at -80°C. Selenomethionine (SeMet)-substituted gp130 D4-D6 was produced in a similar manner, using a metabolic inhibition protocol and LeMaster media supplemented with 50 mg/l L-SeMet (1,2).

Crystallization of gp130 D4-D6 and D1-D6

Crystals of gp130 D4-D6 were obtained by mixing equal volumes of protein (1.2-1.8 mg/ml) with the reservoir solution (12-20% PEG8000, 0.056 M NaCl, 0.1 M Tris-HCl, pH 8.5). Two different crystal forms grew under these conditions, with rod-shaped crystals tending to form at higher PEG and higher protein concentrations, and plates tending to form at lower PEG and lower protein concentrations. Crystallization of SeMet-substituted gp130 D4-D6 was achieved under similar conditions, with the addition of 1 mM tris(2-carboxyethyl)phosphine in all buffers through out the entire purification. Crystals were cryocooled by plunging into liquid nitrogen and X-ray data were collected at 100 K using a nitrogen stream. Prior to freezing, cryoprotection was accomplished by transferring crystals into a solution containing reservoir components plus 25% ethylene glycol.

Crystals of gp130 D1-D6 were obtained by mixing equal volumes of protein at 10 mg/ml with the reservoir solution of 1.5-2.0 M $(NH_4)_2SO_4$, 0.1 M imidazole-malonate buffer, pH 6.0. Cryoprotection was achieved by transferring crystals into a solution containing mother liquid plus 20% ethylene glycol. There was one molecule in the asymmetric unit with unusually high solvent content (78%). There is no observed electron density for residues Glu1, Leu79, Ile83, Glu90, Gly101 and last seven residues 591-597.

Gel filtration chromatography

The native molecular mass of purified D4-D6 was estimated by gel filtration chromatography using a Superdex 75 HR column (GE Healthcare) equilibrated with 20 mM Tris-HCl, pH 7.5. The column was calibrated with Vitamin B12 (1.3 kDa), myoglobin (17 kDa), carbonic anhydrase (29 kDa), ovalbumin (44 kDa), bovine serum albumin (66 kDa), γ-globulin (158 kDa) and thyroglobulin (670 kDa). An elution volume parameter (K_{av}) was calculated for each of the calibration proteins and a calibration curve constructed. By calculating K_{av} for D4-D6 the apparent molecular weight was established.

Supplemental Figures and Legends

Supplemental Table 1. GP130 data collection and refinement statistics.

Numbers in brackets represent statistics for highest resolution shell.

	D4-D6 Monomer		D4-D6 Dimer	D1-D6
Data Collection				
Space group	$P2_12_12_1$		C2	$P2_1$
Cell Dimensions				
a, b, c (Å)	41.6, 75.3, 107.2		102.9, 89.2, 106.9	88.6, 51.8, 166.6
α, β, γ (°)	90.0, 90.0, 90.0		90.0, 117.7, 90.0	90.0, 102.2, 90.0
	Inflection	Remote		
Wavelength (Å)	0.9798	0.9537	0.95443	0.95369
Resolution	50.00-2.00	50.00 – 1.90	50.00-3.05	44.54-3.60
Range (Å)	(2.07-2.00)	(1.97-1.90)	(3.16-3.05)	(3.79-3.60)
R_{merge} (%)	10.8 (57.2)	11.7 (65.7)	15.8 (61.3)	15.3 (134)
$I/\sigma(I)$	28.5 (4.9)	35.3 (4.3)	9.9 (3.0)	7.8 (1.1)
Completeness (%)	100.0 (99.9)	99.8 (98.2)	99.9 (99.3)	99.9 (99.7)
Redundancy	13.3 (10.3)	18.5 (13.9)	3.7 (3.5)	
Refinement				
Resolution (Å)		38.75-1.90	35.15-3.05	44.54-3.60
No. reflections R_{work}		27159	15678	16835
No. reflections R_{free}		2132	791	905
R_{work} (%)		17.77	21.26	26.1
R_{free} (%)		22.03	26.47	32.9
R.m.s. deviations:				
Bond lengths (Å)		0.008	0.002	0.021
Bond angles (°)		1.147	0.621	2.282

Supplemental Figure 1: Snapshots of electron density.
(A) D1-D6, 3.6 Å structure; (B) D4-D6 1.9 Å structure.

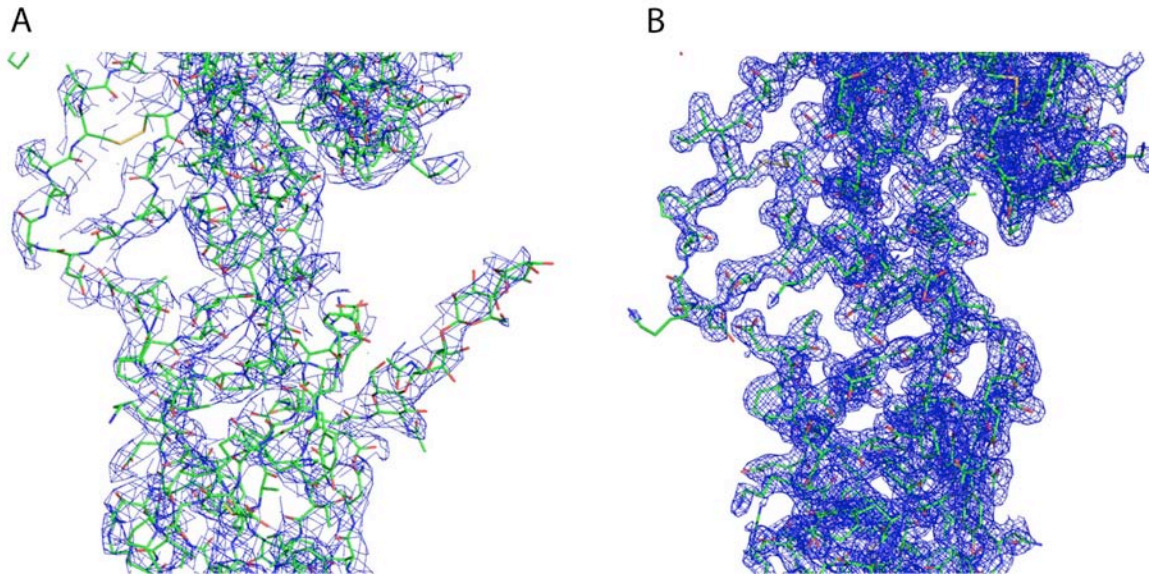

Supplemental Figure 2: Orientation of Ig-like domain D1.
The comparison was made by aligning D2-D3 of gp130 D1-D6 (green) with the published crystal structures of vIL-6/gp130 complex (red, (3)) and IL-6/IL-6Rα/gp130 (blue, (4)). The structure of D1 itself is essentially unaltered but the orientation of D1 in the unliganded gp130 differs slightly from that of D1 in the published structures.

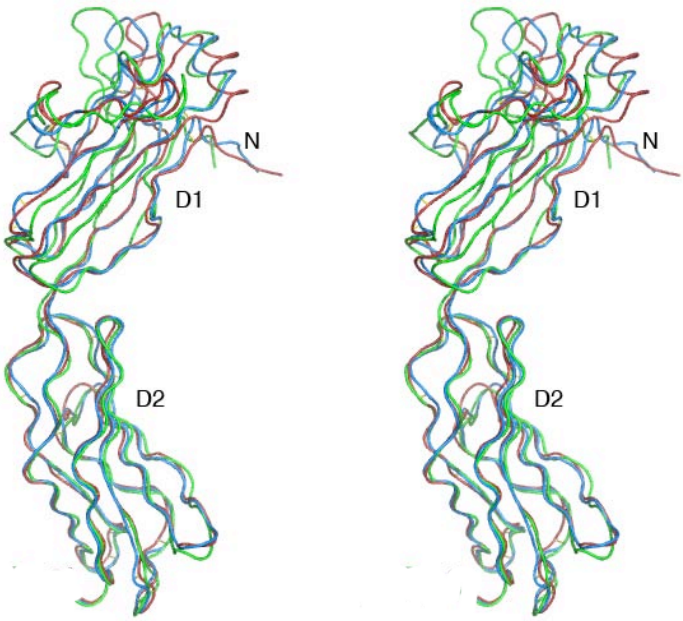

Supplemental Figure 3:
(A) Standard fibronectin-type III domain strand labeling depicted using D4 of gp130.
(B) Sequence alignment of human gp130, residues 260-542, with other members of the human "tall" receptor family. Gp130 b-sheet secondary structure indicated by labeled arrows below the sequence alignment, color-coded as in part (A). Residues of interest noted in the text are highlighted using the same domain coloring as in Figure 1. ∗ indicates homologous residues. Grey box indicates location of disulfide-linked cysteines. Accession codes: gp130 gi 28610147, LIFR gi 4504993, OSMR gi 4557040, TCCR gi 116242518, G-CSFR gi 89954537, IL-12Rβ gi 4504643, IL-31Rα gi 74730327, LR gi 116242617.

A.

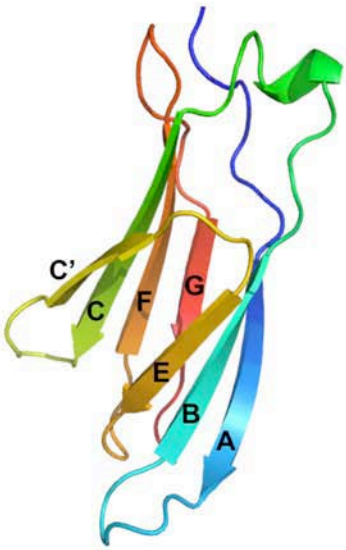

B.

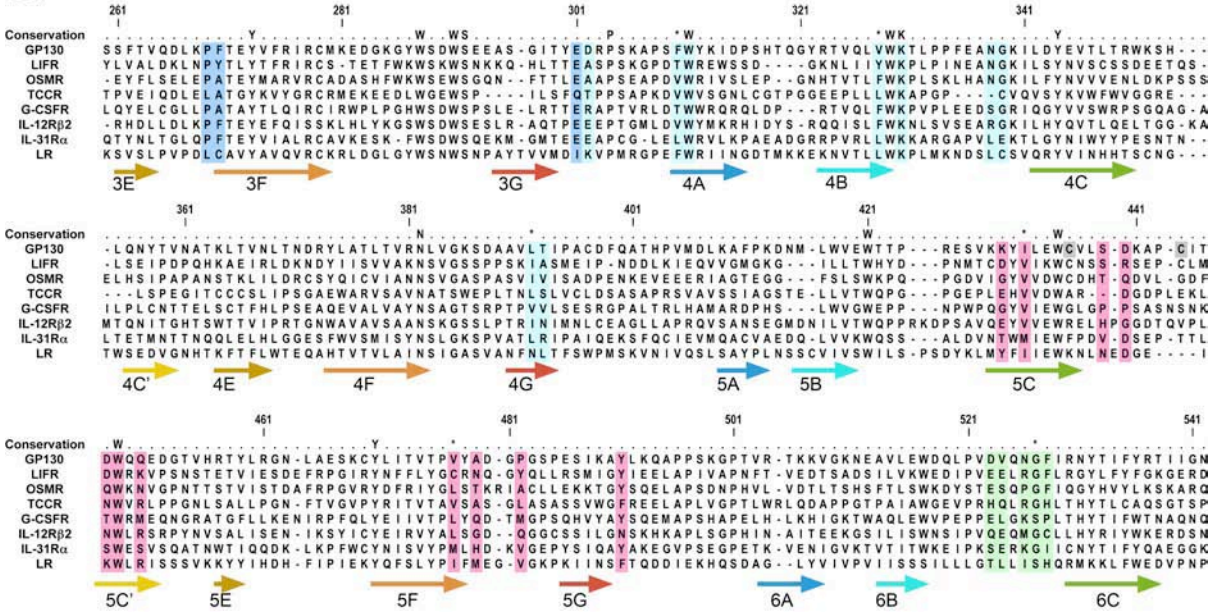

Supplemental Figure 4: Details of the D3/D4 interface.
(A) Crystal packing around the D3/D4 interface. D3 and D5 of gp130 D1-D6 clamp either side of D6 from a symmetry-related molecule. Note that the same packing of D5 against D6 from a symmetry related molecule does not occur in the D4-D6 structures. (B) Overlay of gp130 D3-D4 structure with those of integrin β4 (liganded, 3F7Q (6) in yellow and unliganded, PDB 1QG3 (5) in grey) and type IIB receptor tyrosine phosphatase (PDB 2V5Y (7) in pink, FNIII domains 2 and 3).

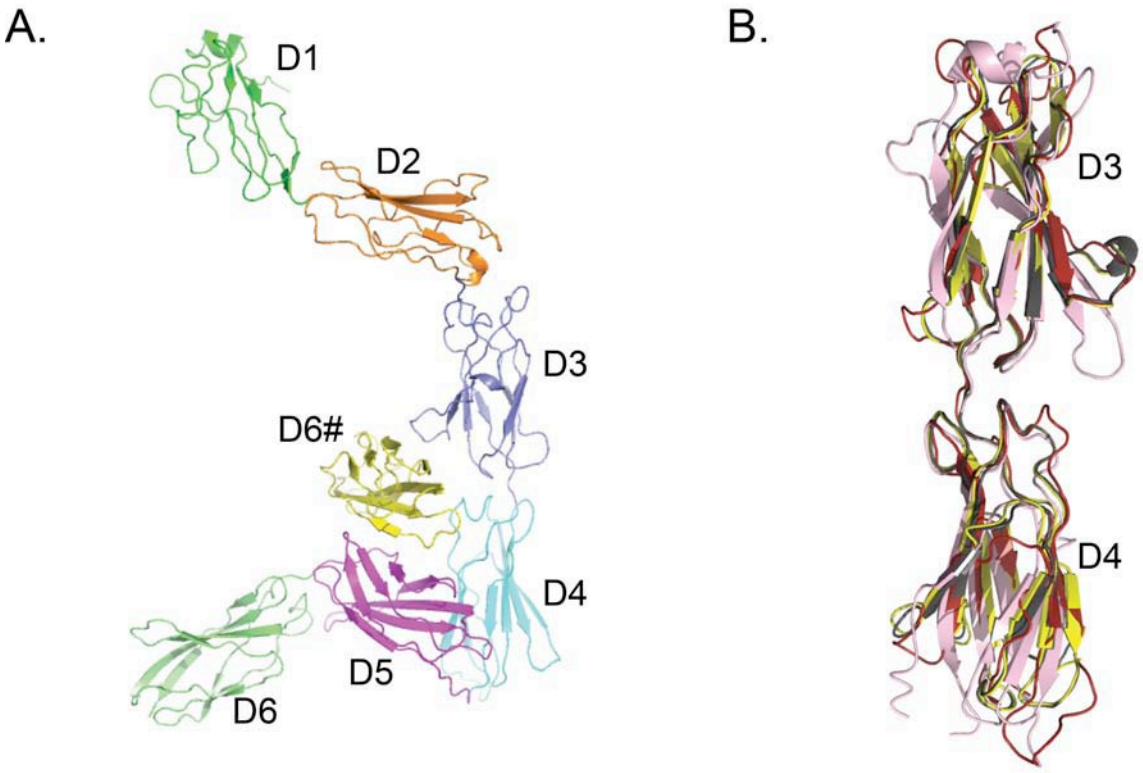

Supplemental Figure 5: Structural model of the extracellular IL-6/IL-6Rα/gp130 hexameric complex and comparison with published electron micrographs.
(A) The structural model was constructed by superposing the structure of gp130 D1-D6 on the crystal structure of the IL-6/IL-6Rα/gp130 D1-D3 hexameric complex (4) by aligning gp130 D2-D3 of these two structures. (i) "Front" view, (ii) and (iii) "Side" views following 45° and 90° rotation, respectively, along the vertical axis of the "front" view shown in (i). IL-6, green; IL-6Rα, blue, gp130 D1-D6, red. In this model, the transmembrane regions of gp130 would enter the membrane approximately 65 Å apart.
(B) A model structure of the complex was reconstructed using the "legs" region from D4-D6 in the monoclinic crystal by aligning D4 of a D4-D6 molecule with D4 of the D1-D6 structure, showing that the transmembrane "legs" regions could be brought together to enter the membrane ~30 Å apart. Models were generated using PyMol (http://www.pymol.org).
(C) EM images from Skiniotis *et al.*, Nat Struct Mol Biol 2005 **12**:545-551 (Reproduced with permission from Nature Publishing Group). Representative class averages of the IL-6/IL-6Rα/gp130 D1-D6 hexameric complex as observed by electron microscopy.

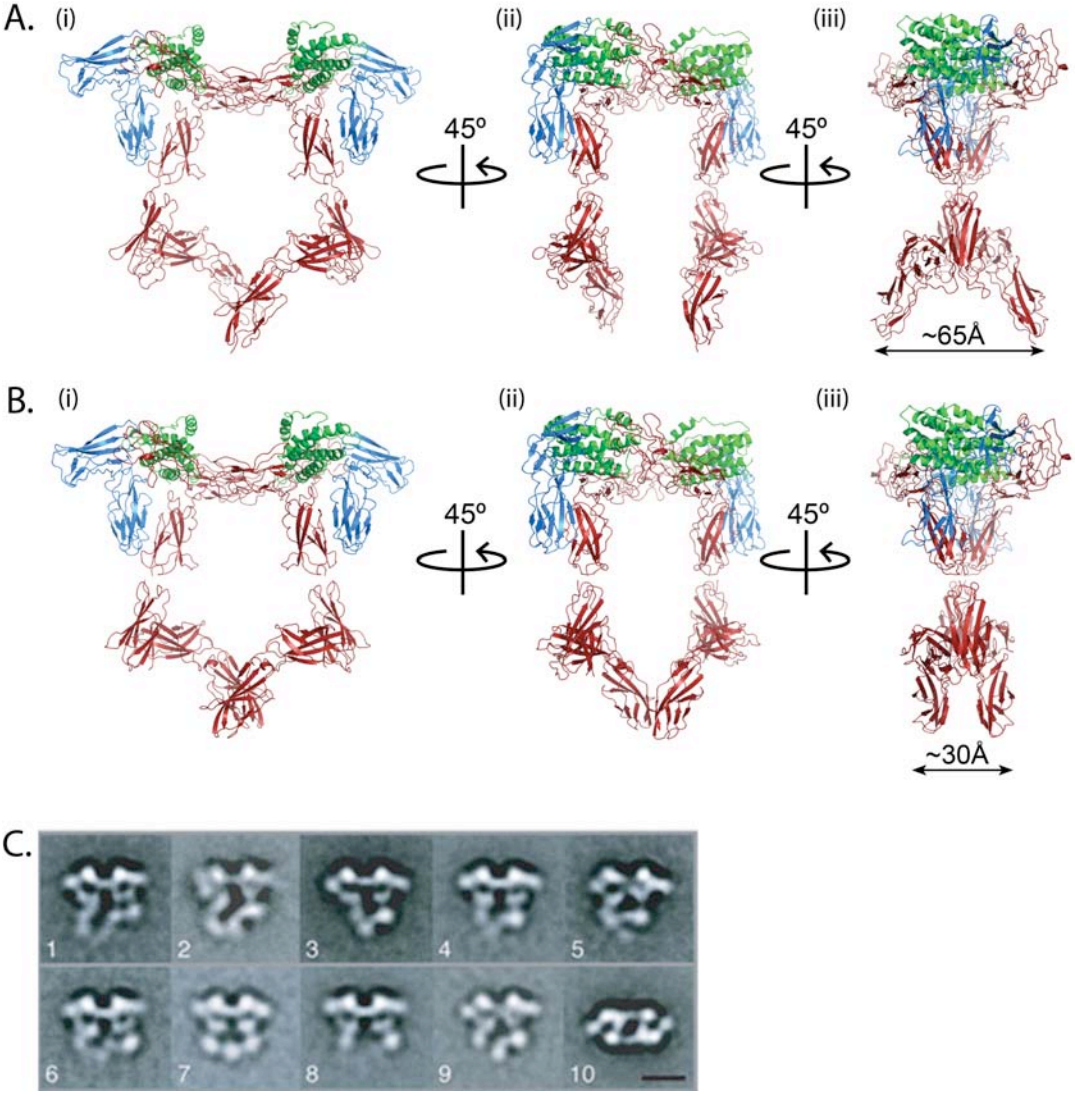

Supplemental Figure 6: D4-D6 is monomeric in solution
Samples of purified D4-D6 at two concentrations (9.0 mg/ml and 1.6 mg/ml) were analyzed by gel filtration chromatography as described above. The protein was eluted with an elution volume of ~11.6 ml, corresponding to an apparent molecular weight of 32,000. The expected molecular mass of the D4-D6 monomer is 35 kDa, suggesting that it is monomeric in solution at both concentrations.

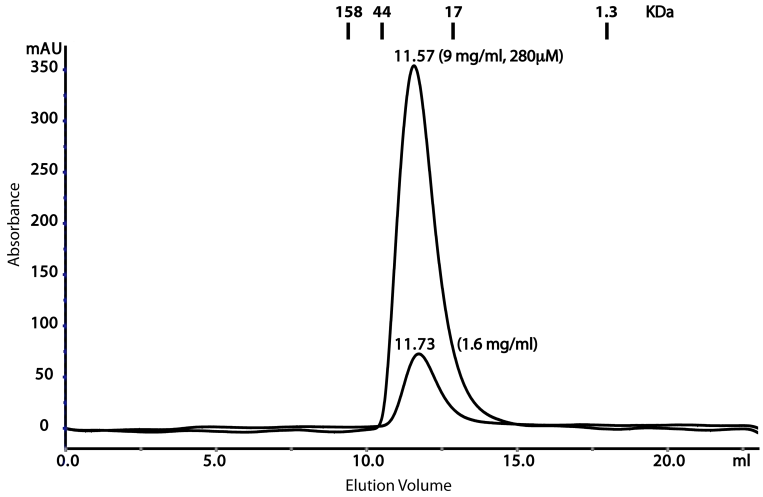

Supplemental References

1. Hendrickson, W. A., Horton, J. R., and LeMaster, D. M. (1990) *Embo J* **9**, 1665-1672
2. Doublie, S. (1997) *Methods Enzymol* **276**, 523-530
3. Chow, D., He, X., Snow, A. L., Rose-John, S., and Garcia, K. C. (2001) *Science* **291**, 2150-2155
4. Boulanger, M. J., Chow, D. C., Brevnova, E. E., and Garcia, K. C. (2003) *Science* **300**, 2101-2104
5. de Pereda, J. M., Wiche, G., and Liddington, R. C. (1999) *Embo J* **18**, 4087-4095
6. de Pereda, J. M., Lillo, M. P., and Sonnenberg, A. (2009) *Embo J* **28**, 1180-1190
7. Aricescu, A. R., Siebold, C., Choudhuri, K., Chang, V. T., Lu, W., Davis, S. J., van der Merwe, P. A., and Jones, E. Y. (2007) *Science* **317**, 1217-1220